Raney copper catalysts for the water-gas shift reaction: I. Preparation, activity and stability

J.R. Mellor[1,a], N.J. Coville[a,*], A.C. Sofianos[b], R.G. Copperthwaite[2,a]

[a]Centre for Applied Chemistry and Chemical Technology, Department of Chemistry, University of the Witwatersrand, Private Bag 3, Wits 2050 Johannesburg, South Africa
[b]Catalytic Technology Group, Division of Materials Technology, Council for Scientific and Industrial Research, Pretoria, South Africa

Abstract

Characterisation of partially leached Raney copper catalysts demonstrated that the chemical nature of the reactant surface could be determined by controlling the leaching process. Initial water-gas shift (WGS) activity of the Raney copper catalysts at the stated conditions compared favourably to the co-precipitated and industrial catalyst alternatives due to a similar active phase composition and high metallic copper surface areas. Raney copper catalyst deactivation in a poison-free environment was attributed to copper crystallite sintering, primarily as a result of a zinc oxide deficiency. Long term (850 h) stability of the Raney catalyst is reported for the first time. Stability improved significantly with increased ZnO loading as a result of better contact between the copper surface and ZnO crystallites. The stabilizing effect of incorporated zinc was independent of its original source. The role of aluminium was to produce Raney copper of high surface area. No beneficial effects of residual alumina in the active catalysts were observed. © 1997 Elsevier Science B.V.

Keywords: Water-gas shift reaction; Raney catalyst; Copper catalyst; Synthesis; Sintering

1. Introduction

Whilst the water-gas shift (WGS) reaction $(CO+H_2O \rightleftharpoons CO_2+H_2)$ is a well established industrial process, studies on water-gas shift catalysts that have high activity, structural stability and sulphur poisoning insensitivity are still on-going [1–7]. Further, uncertainty exists with regard to both the nature of the active sites and the role of additional components such as zinc oxide, alumina and/or chromia in the low temperature WGS catalysts. Thus, debate still continues as to whether the reaction occurs primarily on metallic copper or on isolated Cu(I) cations dissolved in the ZnO lattice [8–14]. The zinc oxide has been proposed to stabilize copper cations in the zinc oxide matrix [8], to create a synergetic effect with the metal copper sites [9,15], or to act as a support for finely divided copper [16].

The ability to prepare a Raney copper catalyst with a surface composition similar to the conventional co-

*Corresponding author.
[1]Present address: Anglo American Research Laboratories (Pty) Limited, PO Box 106, Crown Mines 2025, South Africa.
[2]Present address: Research and Development Department, AECI (Pty) Limited, Private Bag X2, Modderfontein 1645, South Africa.

precipitated low temperature shift catalyst suggests that a Raney copper system should also be active for the WGS reaction [17] and methanol synthesis [18]. Although Raney catalysts have long been known [19,20], it was not until 1980 that the activity of a zinc promoted Raney copper catalyst for *methanol synthesis* was demonstrated by Wainwright and co-workers [18,21]. They also suggested that to a certain extent Raney copper simultaneously promoted the WGS reaction during methanol synthesis. Wainwright and co-workers [22] have since made an on-going study of all aspects of Raney copper–zinc catalysts with particular emphasis on methanol synthesis.

The identification, characterisation and activity of novel Raney copper catalysts for the WGS reaction are reported in this paper. The objective was to determine the requirements for the production of highly active and stable Raney catalysts by the caustic extraction of copper–zinc–aluminium alloys. Specifically, the influence of zinc as a stabilising promoter on WGS activity and long term catalyst stability has been examined. Zinc concentration in the Raney catalyst was varied by controlling the time of contact between the alloy and caustic solution (leach time) [23–25], or by zinc enrichment due to the enhanced precipitation of zinc from zincate added to the leach solution. The effect of precipitated zinc enrichment on Raney copper activity and stability was evaluated with reference to catalyst morphology. For these reasons an extensive analysis of the catalyst morphology as a function of synthesis variables has been undertaken. The continuous sponge-like Raney copper rim (i.e. leached region) suggested that the system may have unique stability characteristics. A co-precipitated and industrial copper-based WGS catalyst were tested under similar conditions for comparison.

2. Experimental

2.1. Catalyst preparation

Alloys, Raney copper catalysts and a co-precipitated catalyst were prepared according to the described methods. Characterisation and activity studies were conducted on Raney catalysts prepared from 0.5 to 1.18 mm alloy particles with nominal composi-

tions of Cu(35) Zn(15) Al(50), referred to as Alloy A and Cu(50) Al(50), referred to as Alloy B.

2.1.1. Alloy preparation

The Cu–Zn–Al and Cu–Al alloys were prepared by Metex (Pty) Limited South Africa, using high purity metals (conductivity grade copper >99% purity, zinc thermal spray wire >99.8% purity and aluminium thermal spray wire >99.5% purity) melted in an AC50 silicon carbide crucible, using a gas fired furnace.

Two methods of preparation were adopted. The Cu–Al binary alloy was prepared by firstly melting the required amount of copper and then adding the required aluminium. The alloy melt was stirred thoroughly and rapidly quenched by pouring into agitated cold water. In some cases, a similar procedure was adopted to prepare the Cu–Zn–Al ternary alloys. A Cu–Al melt was made as described above, and cooled to below 420°C (melting point of zinc) before the required amount of zinc was added to the melt. This procedure helped to prevent rapid vaporisation of the lower melting zinc metal. Rapid stirring and cold water quenching of the melt completed the process.

The second method involved the preliminary formation of Al–Zn and Al–Cu precursor alloys, which, taken in required proportions were melted together, vigorously stirred and rapidly quenched in cold water. The alloy product, in the form of prills ±50×5 mm were crushed using a Christie–Norris hammer mill and screened to provide a product range up to 2 mm in diameter.

The alloys were chosen with 50 nominal wt% aluminium which corresponds to a product with a maximum amount of the primary precipitate $CuAl_2$ reported [26] to be the leachable phase that produces Raney copper. The nominal alloy compositions plotted on the Al–Cu–Zn liquidus projection diagram [26,27] are consistent with this composition.

2.1.2. Caustic leaching

Raney copper catalysts were prepared from the alloys by a procedure similar to that adopted by Friedrich et al. [28]. In these experiments, 20 g of alloy particles 0.50–1.180 mm in diameter were placed in 111 g of de-ionized water at 50±3.5°C. A solution containing 111 ml of 14.1 M aqueous sodium hydroxide solution was added dropwise over 1 h to

achieve a final leach concentration of 7.06 M. Extraction times used in the preparation of the catalysts from Alloy A were 1.0; 1.5; 2.0; 3.0 and 19.5 h. Alloy B was extracted for 1.5 h. The catalyst particles were then thoroughly washed with de-ionized water until the pH of the wash water was 7. The Raney copper catalyst was then dried in air at 120°C for 1 h. Prior to testing, Raney catalysts were re-sieved in order to remove small copper fines generated during the leach reaction.

2.1.3. Zinc impregnation

Varying concentrations of zinc impregnated Raney copper catalysts were produced by leaching Alloy A particles of diameter 0.5–1.180 mm for a total extraction time of 2 h (at 50°C) in solutions of either 0.1, 0.5 or 0.75 M sodium zincate in 7.1 M sodium hydroxide, according to the procedure already outlined. The leach solutions were prepared by digesting the required amount of zinc nitrate (A.R. grade, Merck chemicals) in aqueous sodium hydroxide before addition to the alloy–water mixtures. From the X-ray diffraction (XRD) pattern of the 0.5 M zincate/hydroxide leached catalyst, ZnO was identified as the major precipitated product.

2.1.4. Co-precipitation

A co-precipitated Cu–Zn–Al low temperature WGS catalyst was prepared at the CSIR, South Africa, using a procedure outlined by Stiles [29]. After calcination, the fine powdered catalyst precursors were pressed and sieved to obtain a particle size distribution from 0.500 to 1.180 mm. The particles were then loaded into a muffle furnace and calcined in air at 300°C for 7 h.

2.2. Catalyst characterisation

The bulk metal composition of all catalysts was determined by atomic absorption spectroscopy (Varian Techtron AA4). Alloys and catalysts containing Cu, Zn and Al were analysed by exactly matching the composition of standard and sample solutions. The error of determination was ±2 wt%. A Phillips PW 1050 diffractometer was used to determine the crystalline bulk structure. Differential Scanning Calorimetry (DSC) and Thermal Gravimetric Analysis (TGA) was carried out using a Dupont 9900 thermal analysis system linked to a 910 DSC and 951 TGA module.

The thermal analyses were performed under selected atmospheres by use of a gas manifold system. Scanning electron microscopy (SEM) measurements were performed using a JEOL JSM–35CF Scanning Microscope with energy dispersive analysis by X-ray (EDAX) and elemental mapping facilities. EDAX error of determination was 2–5 wt%. Specific copper surface areas were determined by nitrous oxide pulse experiments based on the procedure reported by Evans et al. [30]. Experimentation showed [31] that an accurate determination of the copper surface area can be obtained using either a single, or a number of nitrous oxide pulses at 90°C. A copper atomic density of 1.35×10^{19} atoms/m^2 was used to calculate the specific copper area. Active copper metal dispersion is expressed in terms of the ratio of the total number of surface atoms to the total number of metal atoms present. Copper particle volume–area mean diameter (d_{VA}) was calculated according to the procedure outlined by Anderson et al. [32]. BET surface area measurements were determined using a Carlo Erba Sorptomatic Series 1800 analyser. Pore size distributions were determined from the Kelvin equation using data obtained from the desorption isotherm [33]. Sulphur analysis was performed in a LECO HF 100 Induction Furnace Analyser.

2.3. Catalyst testing

Catalyst batches of 2±0.1 ml (particle size 500–1180 μm) were tested for activity and stability in stainless steel laboratory microreactors. A conventional stainless steel evaporator and reactor design were employed [31]. Water was fed to the evaporator (at 120°C) using a peristaltic pump. The water vapour was mixed in the evaporator with the carbon monoxide–nitrogen feed gas (purity greater than 99.9%) and the gas–vapour mixture passed into the fixed bed laboratory microreactor via heated lines (110°C). Gaseous products from the reactor were quantified using the thermal conductivity detector (TCD) of a Hewlett Packard 5730A gas chromatograph.

Raney and co-precipitated copper-based catalysts were reduced according to a similar procedure. The catalysts were firstly heated in inert N$_2$ to 120°C at a rate of 50°C/h. A premixed 5% H$_2$/N$_2$ (by volume) gas was substituted at a gas hourly space velocity (GHSV) of 900 h^{-1} and reduction commenced. The catalyst

temperature was increased to a maximum of 230°C at 30°C/h and maintained for 16 h. At all stages of reduction, care was taken to prevent exothermic temperature run-aways. After reduction, the catalysts were cooled to 200°C and the reactor flushed with N_2 prior to the introduction of reagent gases. The WGS activity was evaluated at 200°C with a CO : H_2O ratio of 1 : 22.5. The dry gas composition was 10% CO/90% N_2. A total GHSV of 1000 h^{-1} was maintained. Catalyst testing was conducted at atmospheric pressure (620 mm/Hg). Blank thermal reactions in the absence of catalysts were found to be negligible, as was the formation of iron carbonyls in the stainless steel reactors.

3. Results and discussion

3.1. Characterisation

3.1.1. Bulk structure

The bulk analysis of the Alloys A and B of nominal composition Cu(35) Zn(15) Al(50) and Cu(50) Al(50), respectively, the caustic leached catalysts, an industrial catalyst and a co-precipitated WGS catalyst were determined by AA spectroscopy and the results are presented in Table 1. AA analysis also revealed no change in catalyst composition after WGS reaction. As the catalyst rim could not be accurately removed from the alloy core for separate AA analysis (see Fig. 1), semi quantitative chemical compositions for the reacted rims and cores were calculated from at least two representative EDAX measurements, and the results are given in Table 1. As can be seen significant

variations in the Cu, Zn, Al content of the two parts of the particles were observed.

Catalyst particles were found to be roughly spherical whilst the alloy surface was non-uniform, and not very porous. In some cases cracks and fissures were apparent and are considered to form during rapid quenching of the melt or from the stress associated with alloy crushing to obtain required particle sizes. Extensive rearrangement of the copper occurred on occasion during leaching [34,35] and this gave rise to the formation of the copper rich nodules on the dendritic leached structures.

The morphological development of 'fresh' Raney catalysts prepared by varying the alloy contact time to caustic solution were monitored by electron micrographs and are shown in Fig. 1. For all extraction times investigated, a boundary parallel to the original alloy surface, was observed. Partial leaching of alloys (for 1.5 and 2 h) resulted in reaction product zones consisting of two layers, an outer layer of light coloured sponge material with interspersed black areas, and an inner band of intermediate shading of average diameter (30–40 μm) which is independent of alloy leach depth [36]. Microprobe analysis showed that the grains of the outer layer were essentially copper, whilst those in the inner layer were unreacted $Cu(Zn)Al_2$. After 3 h no core was distinguishable from a rim, indicating that the particle had been leached to the centre. By contrast, Andreev et al. [35] reported that the centre of a particle of diameter 1.2–2 mm and chemical composition Cu(42.0) Zn(14.3) Al(43.5) was stable to leaching as a result of the ordered crystalline structure formed by slow quenching during alloy formation.

Table 1
Compositions of Raney copper catalysts after varying leach times

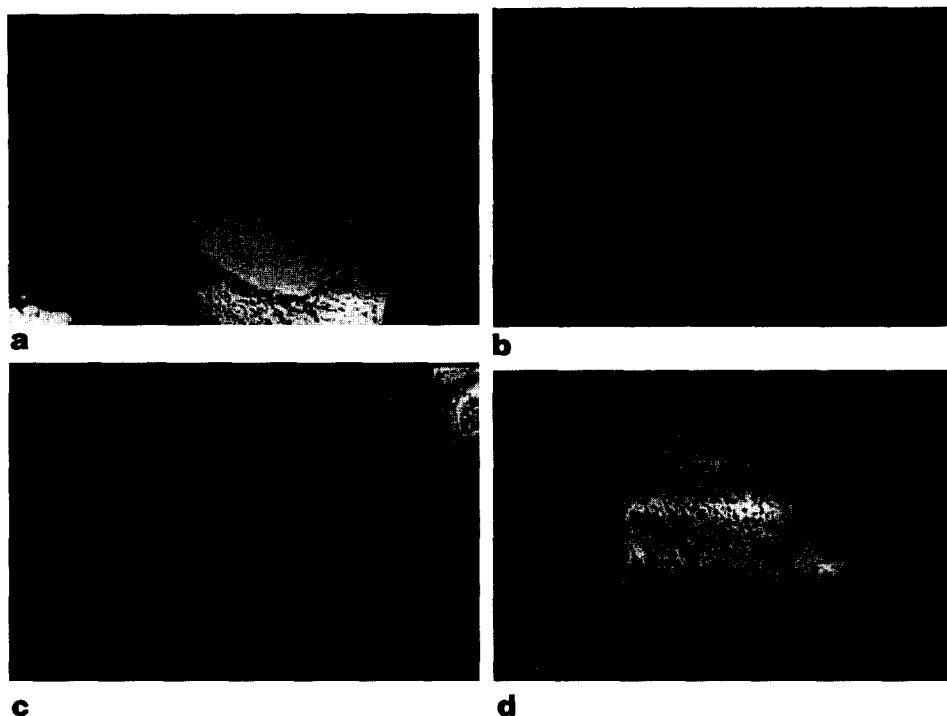| Sample	Extraction time (h)	Composition (wt%)			Rim (wt%)			Core (wt%)		
		Cu	Zn	Al	Cu	Zn	Al	Cu	Zn	Al
Alloy A	1.0	69.2	6.1	21.7	83.4	9.9	6.7	37.7	11.6	50.7
Alloy A	1.5	73.8	5.3	16.3	90.0	3.8	6.2	40.3	14.3	45.7
Alloy A	2.0	76.1	3.2	19.7	90.1	2.9	6.9	39.5	14.2	46.4
Alloy A	3.0	84.6	1.8	11.6	88.8	0.0	11.2	a		
Alloy A	19.5	87.0	1.4	6.8						
Alloy B	1.5	84.7	0.0	15.3	91.8	0.0	8.2	a		
Industrial		25.8	31.5	17.9						
Precipitated		12.4	31.7	15.6						

[a] No core observed from SEM.

Fig. 1. Cross-sectional electron micrographs of Alloy A leached for (a) 1.0, (b) 1.5, (c) 2.0 and (d) 3.0 h.

There is no evidence in the *unused* catalyst of any mechanical structure collapse or damage brought about by the leach action to produce a powdery material. Thus, changes in pore structure, pore volume and surface area cannot be attributed to such an effect. However, crystallite shape changed with increasing leach time. Granular shapes are observed up to a leach time of 1.5 h, after which longer times result in more elongated 'needle like' crystallites.

Identification of the bulk phases in Alloys A and B and their corresponding changes as a function of leach time was conducted using XRD analysis. The diffraction patterns of *Alloy A* and 1 and 3 h leached catalysts before and after testing, are shown in Fig. 2(a)–(e). The diffraction patterns of *Alloy B* and 1.5 h leached catalysts before and after testing are presented in Fig. 3(a)–(c). Diffraction patterns for the fresh co-precipitated and industrial catalysts was also performed but here only CuO could be identified from XRD patterns. Both Alloys A and B have the binary $CuAl_2$ phase as their primary precipitate. It is possible that this phase may be represented as $Cu(Zn)Al_2$ for

Alloy A as it is known that the $CuAl_2$ phase can dissolve 2–3 wt% Zn with little change in lattice parameters [27,37]. Alloys A and B show well resolved patterns indicating the binary CuAl phase and an Al solution as secondary products. A larger abundance of the CuAl phase is seen in Alloy B due to its closer 'proximity' to the CuAl phase constitution than that of Alloy A. No evidence of the ternary phases $T=Cu_5Al_3Zn_2$ and $T=Cu_3Al_3Zn$ previously identified by XRD in similar Cu–Zn–Al alloy compositions by Bridgewater et al. [38] were found. Also, the XRD analysis did not reveal the presence of α-brass which has been reported to be formed in Cu–ZnO catalysts for the WGS reaction [39].

The morphology of Raney copper catalysts is produced by caustic leaching which proceeds in three stages [37]. In the *first stage* (times up to 1.5 h) leaching of the $CuAl_2$ phase and Al solid solution from Alloy B leads to the formation of a *fully extracted alloy* with copper containing traces of Al. Thus, the addition of Zn to the precursor alloy has the effect of slowing the rate of the leach reaction. The
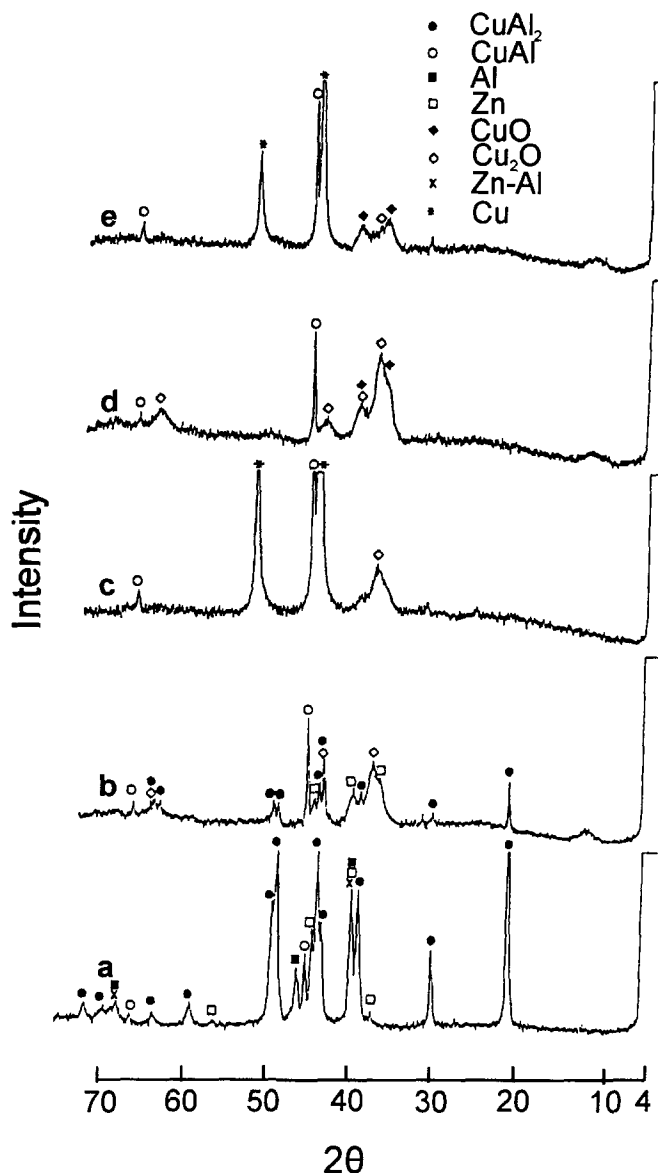
Fig. 2. XRD patterns of fresh and used Raney copper catalysts produced from leaching Alloy A for various times. (a) Alloy A, no extraction, (b) 1.0 h leach, *before* reaction, (c) 1.0 h leach, *after* reaction, (d) 3.0 h leach, *before* reaction, (e) 3.0 h leach, *after* reaction.

majority of the Cu(Zn)Al₂ phase is evenly leached from the outer rim (see Fig. 1), parallel to the particle boundary, to leave porous Raney copper. For all alloys and leach times, the Al associated with Cu in the CuAl phase, was resistant to caustic attack. No reason for the decrease in reactivity of this material could be determined. After reaction, elemental Cu was predominant in all the Raney catalysts.

In the *second stage* of reaction (times of 2–3 h) repeated analysis showed that there is an overall increase in bulk copper content, with increasing extraction time. The levels of Cu in the leached product (rim) remained relatively constant after 1 h, with a corresponding decline in Zn concentration. The Al content in the leached product steadily increased (from a minimum of 6.2% at 1.5 h to 11.2% after 3 h)
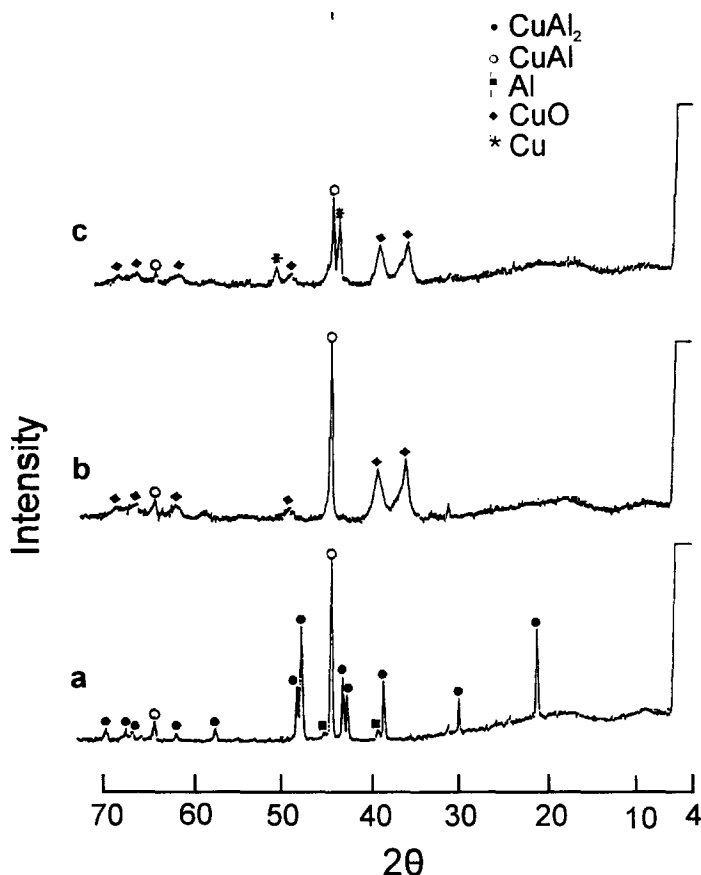
Fig. 3. XRD patterns of fresh and used Raney copper catalysts produced from leaching Alloy B for 1.5 h: (a) Alloy B, no extraction, (b) 1.5 h leach, *before* reaction, (c) 1.5 h leach, *after* reaction.

and remained at relatively high levels until the alloy core of the leaching particle was completely exhausted. This result is only consistent if there is a net transfer of Al from the leaching intergranular solid solution to the $Cu(Zn)Al_2$ phase leach residue [40].

In the third and *final stage* of reaction, the Al content was lowered as the residual soluble metals were removed.

It may be concluded that the nature of Raney copper catalysts will derive from the phase constitution of their precursor alloys and subsequent morphological development which is sensitive to leach time.

3.1.2. Surface structure

The nitrogen isotherms for Raney catalysts produced by leaching Alloy A for 1, 1.5, 2 and 3 h showed a Type A hysteresis loop [41] which is repre-

sentative of cylindrical capillary shapes, as would be expected for the 'striated' needle-like nature of the leached copper product. The BET and copper surface areas, together with crystallite diameter and copper dispersion are presented in Table 2 for catalysts derived from Alloys A and B, as well as the industrial and co-precipitated WGS catalysts. The corresponding pore volumes and mean pore radii for the catalysts described above are also shown in Table 2.

From Table 2 it can be seen that the pore volume increased as the Al and Zn content of Alloy A was depleted, whilst the removal of residual Al and Zn after 19.5 h leaching resulted in the partial elimination of these pores. Pore radii and copper crystallite size (Table 2) increased with increasing extent of leach reaction, which qualitatively confirms the trend. Also, a decrease in pore size after core extraction confirmed

Table 2
Physical properties of the fresh and used Raney copper catalysts after varying leach times[a]

Sample	Extraction time (h)	S_{BET} (m^2 g^{-1})	S_{Cu} (m^2 g^{-1})	Copper crystallite diameter (Å)	Copper dispersion (%)	Pore volume (cm^3 g^{-1})	MPR[b] (Å)
Alloy A	1.0	27.0 (21.5)	15.7 (4.6)	297 (1003)	5.3 (1.8)	0.062 (0.058)	56.9 (53.9)
Alloy A	1.5	33.4 (20.3)	16.9 (2.9)	294 (780)	6.6 (2.4)	0.082 (0.08)	68.7 (75.5)
Alloy A	2.0	32.8 (19.0)	15.8 (10.1)	324 (514)	5.8 (3.7)	0.197 (0.141)	121.2 (184.4)
Alloy A	3.0	28.2 (22.2)	13.7 (9.9)	415 (572)	4.5 (3.3)	0.313 (0.187)	260.6 (324.8)
Alloy A	19.5	10.2 —	7.8 —	750 —	2.6 —	0.26 —	99.5 —
Alloy B	1.5	20.0 (15.8)	10.2 (6.9)	557 (841)	3.4 (2.4)	0.194 (0.164)	122.7 (145.8)
Industrial		81.6 (80.7)	8.2 (7.4)	212 (238)	9.2 (8.1)	0.257 —	69.4 —
Precipitated		85.9 (83.2)	5.3 (7.5)	157 (143)	12.2 (13.5)	0.471 —	203.3 —

[a]Results in brackets for *used* catalysts.
[b]MPR=Mean pore radii.

that pore elimination takes place as a result of the removal of residual metals [34,37].

Total BET surface areas reach a maximum after about 1.5 h leaching time, and then follow a slight decline. A maximum in surface area after approximately 1–2 h leaching has been observed by many researchers, both for leaching Cu–Al alloys [42] and Cu–Zn–Al alloys [43]. A leach depth range 150–300 μm produced a catalyst with excellent catalyst performance (1–1.5 h leaching) which corresponded to a copper surface area which is a maximum and crystallite diameter which is a minimum. Pore radii, although at a minimum at this leach time, are presumably still large enough to support mass transfer effects and do compare to sizes present in co-precipitated and industrial catalysts. For leach times greater than the optimum, both the BET and copper surface areas gradually decrease even though the pore volume of leached material increases (Table 2).

3.1.3. Thermometric analysis of partially leached Raney copper catalysts

The procedure for reducing the Raney copper catalysts (produced from Alloy A and B) under 5% H$_2$/N$_2$ was simulated by DSC in order to supplement the structural information obtained by XRD. The catalyst samples were heated from ambient to 300°C at a rate of 5°C/min in a gas flow of 30 ml/min. The results showed that reduction involved a single *major* exothermic phase change between 165°C and 220°C. *Pure* Cu$_2$O and CuO powdered samples were observed to reduce over a similar temperature range (165–225°C) under the same experimental conditions.

The DSC results are consistent with the XRD analysis (Figs. 2 and 3) which showed that oxidised copper was reduced to elemental copper during the activation procedure.

Since it is known [44] that Raney copper catalysts are susceptible to sintering during reduction, the influence of the stated reduction conditions for catalyst evaluation on the *active* Raney copper surface area under various reducing atmospheres was investigated. Consequently, investigations by DSC at a temperature rate of 5°C/min in currents of pure H$_2$, CO and 5% H$_2$/N$_2$ (at a flow rate of 30 ml/min) were carried out using a 1.0 h leached (Alloy A) Raney catalyst with sample weights up to 15 mg, arranged as a fine layer. Significant loss of surface area was observed when pure H$_2$ (12.1 m^2 g^{-1}) or CO (9.8 m^2 g^{-1}) is used as reductant when compared to 5% H$_2$/N$_2$ (15.7 m^{2}g^{-1}). The greatest loss in surface area corresponded to the highest generated reduction heat in the bed, inferring that sintering of the Raney copper was responsible for loss of surface area [44,45]. The results show that under the stated reduction conditions, reduction in 5% hydrogen in nitrogen maximized the *active* copper surface area of the Raney copper catalysts.

3.2. Activity and stability

3.2.1. Activity

The manner in which *activity data* for Raney copper systems is reported has tended to be varied. Partially leached Raney copper catalysts consist of an extracted rim of active material and a core of unextracted alloy. Although this core does not provide catalytic activity,

Table 3
The bulk density of Raney copper catalysts as a function of leach time and alloy composition

Sample	Extraction time (h)	Density (g ml^{-1})
Cu(35) Zn(15) Al(50)	1.0	1.5
Cu(35) Zn(15) Al(50)	1.5	1.4
Cu(35) Zn(15) Al(50)	2.0	1.34
Cu(35) Zn(15) Al(50)	3.0	1.03
Cu(43) Zn(18) Al(30)	1.0	1.73
Cu(25) Zn(25) Al(50)	1.0	0.88
Cu(10) Zn(40) Al(50)	1.0	0.84
Industrial		0.97
Precipitated		1.0

it does contribute to the composite mass of the catalyst particle. The bulk density of a Raney catalyst particle of unit volume decreases as a function of increasing leach time (Table 3) and decreasing alloy copper content (Table 3). Hence careful interpretation of activity data based on the *mass* of Raney catalysts with varying alloy composition and/or extraction depth must be exercised.

For completeness, and as an illustration of the pitfalls of reporting Raney copper catalyst results, the *initial* activities of the partially leached catalysts of Alloys A and B together with the industrial catalyst and co-precipitated catalyst are presented in different ways in Table 4. Specific activities have been expressed as the rate (per hour) of moles of carbon monoxide converted as a function of: volume of catalyst particles (Rate a), composite (total) mass of catalyst particles (Rate b), specific copper surface area (Rate c) and BET surface area (Rate d).

Expressing activity as a function of constant catalyst volume (Rate a) demonstrates that 'particle for particle' Raney copper catalysts extracted from 1 to 3 h are more active than the industrial and co-precipitated catalysts. As the catalyst *volume* required determines the type and size of reactor needed for a particular catalyst [6], Raney catalysts may present important economical advantages. Raney copper activity (Rate a) decreases with decreasing copper surface areas and increasing crystallite growth as expected. Activity based on the composite mass of the Raney catalyst (Rate b) highlights the variable density phenomenon. Increasing the extent of alloy extraction decreases the catalyst density with a corresponding overall increase in the activity based on composite mass. A comparison of the activities (Rate b) of catalysts with similar bulk densities (Table 3) indicates that on a mass basis the fully extracted 3 h leached Raney copper catalyst (of lowest volume-based activity) displays a higher activity than both the industrial and co-precipitated catalysts. Some authors [37] have attempted to circumvent the variable density problem by expressing activity (for methanol synthesis) in terms of a theoretically calculated mass of 'rim material' since the catalyst activity was suggested to correlate with the copper rim. This method also involves a large number of simplifying assumptions [42]. From the above discussion we propose that meaningful comparisons between potential catalytic systems should be made by *considering the entire catalyst particle*.

The activities of Raney copper catalysts expressed in terms of specific copper surface area (Rate c) are low in comparison to the industrial and co-precipitated catalysts as a result of the high density, copper rich core which ensures a low percentage active metal dispersion (Table 2). However, from Table 4, it can

Table 4
Specific activities of Raney, co-precipitated and industrial catalysts[a]

Sample	Extraction time (h)	Rate (a) ($\times 10^{-3}$ mol$_{co}$/ml/h)	Rate (b) ($\times 10^{-3}$ mol$_{co}$/g$_{comp}$/h)	Rate(c) ($\times 10^{-4}$ mol$_{co}$/m$^2_{Cu}$/h)	Rate(d) ($\times 10^{-5}$ mol$_{co}$/m^2/h)
Alloy A	1.0	3.44	2.30	1.47	8.50
Alloy A	1.5	3.41	2.43	1.44	7.29
Alloy A	2.0	3.44	2.58	1.63	7.86
lloy A	3.0	3.29	3.21	2.34	11.37
Alloy B	1.5	3.37	2.92	2.86	14.61
Industrial		3.06	3.15	3.84	3.86
Precipitated		2.94	2.94	5.55	3.43

[a]Temperature=200°C; total GHSV=1000 h^{-1}; dry gas composition=10% CO/90% N$_2$; CO : H$_2$O=1 : 22.5; catalyst volume=2±0.1 ml.
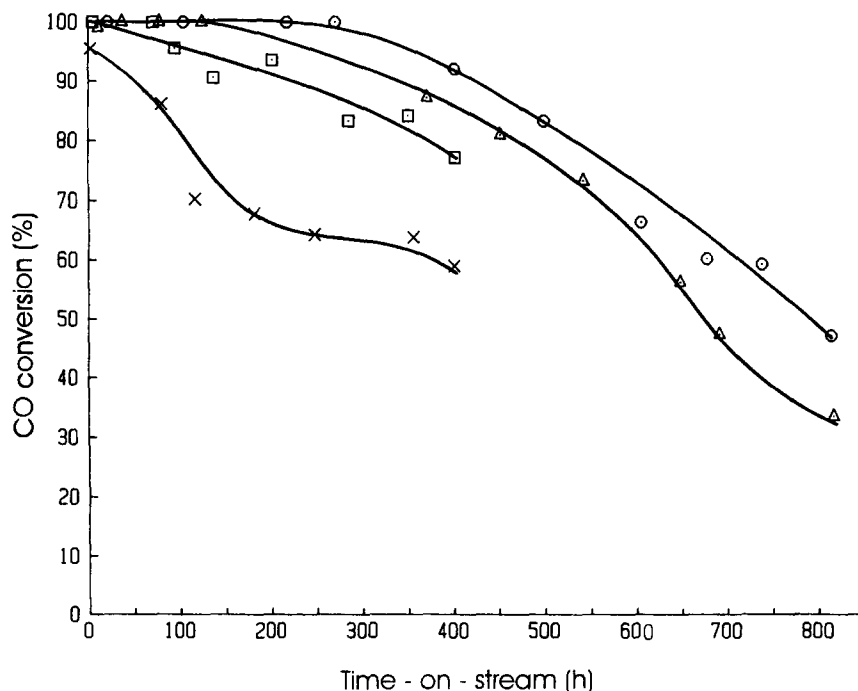
Fig. 4. Stability of various Raney copper catalysts as a function of Alloy A leach time. (Temperature=200°C; total GHSV=1000 h^{-1}; dry gas composition=10% CO/90% N$_2$; CO : H$_2$O=1 : 22.5; catalyst volume=2±0.1 ml) ○=1 h leach, △=1.5 h leach, □=2 h leach, X=3 h leach.

be seen that all Raney copper catalysts evaluated showed a higher total surface area efficiency (Rate d), than the industrial and co-precipitated alternatives. This result is consistent with the findings of Andreev et al. [35] who also noted that the productivity per unit surface area of a Raney catalyst was significantly higher than that of a low-temperature co-precipitated oxide catalyst over a large range of flow rates.

3.2.2. Stability

Little information on the long term activity of Raney copper catalysts for the WGS reaction is available [35]. Friedrich et al. [46] noted that Raney copper for methanol synthesis is resistant to sintering in the short term, and postulated a minimal loss in activity with time-on-stream due to the unique catalyst morphology. No detailed explanations were given for this proposal.

A series of Raney copper catalysts (prepared from Alloy A) were investigated for long term stability in the WGS reaction, and the results are shown in Fig. 4. It can be seen from Fig. 4 that the activity of the Raney copper catalysts had decreased significantly after

850 h-on-stream. In comparison, the industrial catalyst and co-precipitated catalyst showed only minimal decreases over the same time period. No significant levels of sulphur or carbon were present in the used catalysts. Notable decreases in the total surface area (Table 2) of Raney copper catalysts through sintering were, however, observed after the WGS reaction. The copper surface area and average crystallite diameter of the industrial and co-precipitated catalysts remain approximately constant during reaction, hence explaining the catalysts sustained stability.

Analysis of the electron micrographs of the *surface* of 1 and 3 h leached catalysts *after* WGS reaction showed that although the porous nature of the surface had disappeared in both catalysts, but that the integrity of the rim remained unchanged. However, *cross-sectional* electron micrographs clearly revealed the growth of copper 'islands' in the leached rim during reaction of 1 and 3 h leached catalysts. Cross-sectional elemental mapping of the rim of a 1 h leached Raney catalyst *after* reaction revealed no concentration effects of support materials. It would therefore seem unlikely that sintering of copper crystals occurs as a

consequence of the migration of Zn or Al under WGS conditions. This permits us to draw the important conclusion that *Raney copper stability for the WGS reaction decreases with decreasing catalyst zinc content.*

A comparison of the XRD phases of the fully extracted fresh 3.0 h leached Alloy A catalyst and the 1.5 h leached Alloy B catalyst with similar *bulk* copper contents (84.6 and 84.7%, respectively, Table 1) shows that the dominant leach resistant CuAl phase in Catalyst B does not effectively contribute to the specific copper surface area (Table 2). Both catalysts showed similar deactivation profiles and activity losses after 400 h-on-stream, indicating no stabilization effect from the bulk 1.8 ± 1.5 wt% zinc content in the 3 h leached Alloy A catalyst.

3.3. Zinc impregnation

Various concentrations of zinc impregnated Raney copper catalysts were produced by leaching Alloy A for 2 h in solutions of either 0.1, 0.5 or 0.75 M sodium zincate in 7.1 M sodium hydroxide. From the XRD pattern of the 0.5 M zincate/hydroxide leached catalyst, zinc oxide was identified as the major precipitated product. AA analysis of the various catalysts (Table 5)

reveals that a higher concentration of zinc in the leach solution corresponds to a greater deposition of zinc into the Raney copper catalyst [23]. Cross-sectional EDAX analysis of the 0.5 M zincate leached catalyst showed a 7.2 times zinc excess in the rim compared to a catalyst produced with no zincate added to the caustic leach solution (Table 5).

The total BET and copper surface areas together with copper crystallite diameters of the zincate/hydroxide leached catalysts are presented in Table 6. Corresponding pore volumes and mean pore radii are also given in Table 6. Total BET surface area was observed to decrease with increasing zincate concentrations in sodium hydroxide (and zinc loading) for similar leach conditions [25,37]. Adding increasingly concentrated zincate to the caustic leach solution effectively slows the rate of reaction (for a constant leach time) causing a change in the leaching behaviour. Pore volume and pore radii were observed to generally decrease with decreasing leach rate (Table 6). The lower leach rates promoted an increase in copper crystallite size which consequently resulted in a loss of surface area in the leached copper structures [47]. *The leaching process in zincate/hydroxide solutions is therefore regarded as the fundamental determinant of catalyst surface morphology.*

Table 5
Compostion of zinc impregnated Raney copper catalysts

Zincate conc. (M)	Extraction time (h)	Composition (wt%)			Rim (wt%)			Core (wt%)		
		Cu	Zn	Al	Cu	Zn	Al	Cu	Zn	Al
0	2.0	76.1	3.2	19.7	90.1	2.9	6.9	39.5	14.2	46.4
0.1	2.0	74.9	5.4	17.6						
0.5	2.0	71.9	8.1	18.6	74.6	21.0	4.4	40.4	13.8	45.9
0.75	2.0	63.2	14.7	20.8						

Table 6
Physical properties of fresh and used zinc impregnated Raney copper catalysts[a]

Zincate conc. (M)	Extraction time (h)	S_{BET} (m^2 g^{-1})	S_{Cu} (m^2 g^{-1})	Copper crystallite diameter (Å)	Pore volume (cm^3 g^{-1})	MPR[b] (Å)
0	2.0	32.8	15.8 (10.1)	324 (514)	0.197	121.2
0.1	2.0	28.2	14.6 (9.7)	345 (519)	0.150	133.6
0.5	2.0	23.9	11.3 (9.1)	428 (531)	0.027	127.8
0.75	2.0	9.5	4.2	1012	0.028	116.2

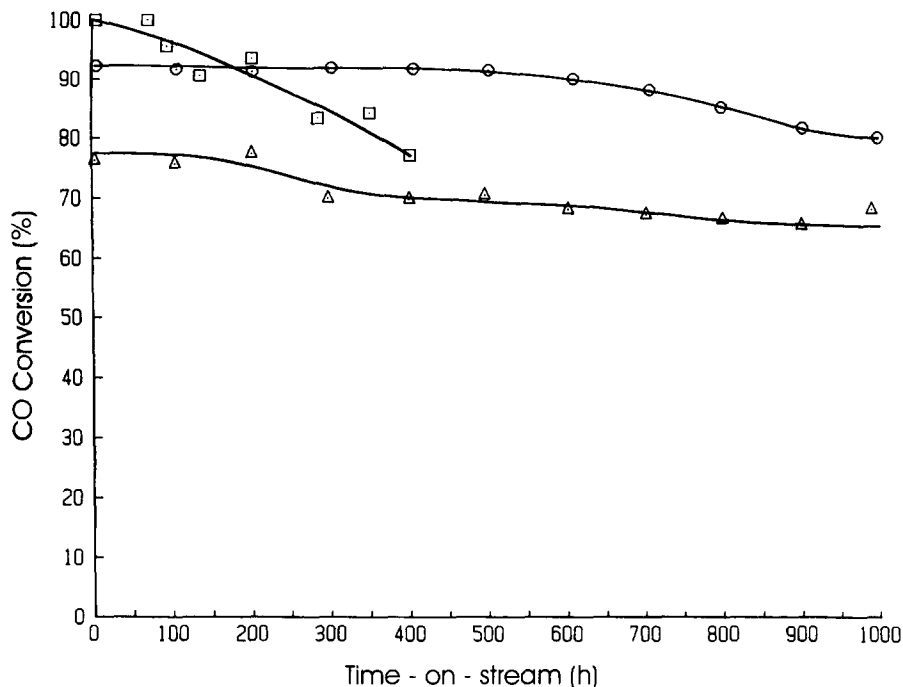[a]Results in brackets for *used* catalysts.
[b]MPR=Mean pore radii.

Fig. 5. Stability of zinc impregnated Raney copper catalysts. (Temperature=200°C; total GHSV=1000 h^{-1}; dry gas composition=10% CO/ 90% N$_2$; CO : H$_2$O=1 : 22.5; catalyst volume=2±0.1 ml) □=No zincate added to caustic solution; ○=0.1 M Zincate; △=0.5 M Zincate.

The initial activity and stability of Raney copper catalysts produced from leaching Alloy A for 2 h in varying zincate concentrations is shown in Fig. 5. The figure clearly indicates the beneficial effects of leaching in zincate solutions, a result similar to that found for Raney catalysts used in the methanol synthesis reaction [25]. From Fig. 5 it can also be seen that while improving the stability of copper crystallites, deposited zinc oxide also causes a decrease in initial catalyst activity due to the smaller surface areas of Raney copper catalysts resulting from leaching in caustic solutions with high concentrations of zincate.

This effect of ZnO on Cu/Al WGS reaction catalysts is consistent with other literature reports. For example, in a previous study reported by us [48], zinc ions were implanted into the surface of a partially leached Cu(50) Al(50) alloy by ion implantation procedures. In this experiment, zinc oxide was observed to assist in the process of stabilizing copper crystals by acting as a suitable spacer material. Long term stability was found to be related to the amount of zinc present in the catalyst.

4. Conclusion

Caustic leached Raney copper catalysts with rim compositions of Cu–ZnO–Al$_2$O$_3$ were identified as highly active low temperature WGS catalysts. The nature of the reactant surface area, crystallite size, pore volume and pore radii was determined by the leaching conditions. Our preliminary findings suggest that WGS activity is dependent, at least in part, on the copper surface area.

Although initial WGS activities were comparable to the industrial and co-precipitated catalyst, deactivation as a result of copper crystallite sintering took place over long operating times. Catalyst instability resulted from a rim zinc oxide deficiency. Presumably even greater amounts of zinc for long term catalyst stability could be provided by the impregnation process. However, the addition of concentrated zincate to the caustic solution also slowed the leach rate, promoting an increase in copper crystallite size with a corresponding decrease in copper surface area and WGS activity. In a second paper dealing with the of

Raney copper catalysts [49], further contributory roles of ZnO to Raney copper WGS performance are considered.

Acknowledgements

References

[1] D.S. Newsome, Catal. Rev. Sci. Eng. 21 (1980) 275.
[2] S. Strelzoff, Technology and Manufacture of Ammonia, Wiley, New York, 1981, p. 1.
[3] H. Bohlbro, M.H. Jorgensen, Chem. Eng. World 5 (1970) 46.
[4] F.M. Gottschalk, R.G. Copperthwaite, M. van der Riet, G.J. Hutchings, Appl. Catal. 38 (1988) 103.
[5] L. Lloyd, M.V. Twigg, Nitrogen 188 (1979) 30.
[6] W.J. Lywood, L. Lloyd, D.E. Ridler, M.V. Twigg, in: M.V. Twigg (Ed.), Catalysis Handbook, 2nd ed., Wolfe Publishing, London, 1989.
[7] C. Rhodes, G.J. Hutchings, A.M. Ward, Catal. Today, 23 1995.
[8] G. Petrini, F. Montino, A. Bossi, F. Garbassi, in: G. Pancelet (ed.), Preparation of Catalysts 3, Elsevier, Amsterdam, 1983.
[9] R.G. Herman, K. Klier, G.W. Simmons, B.P. Finn, J.B. Bulko, J. Catal. 56 (1979) 407.
[10] P. Stefanov, Ts. Marinova, N. Kasabova, D. Shishkov, I. Risha, Compt. rend. Acad. Bulg. Sci. 23 (1990) 370.
[11] D.K. Ghorai, N.C. Ganguli, S.P. Sen, Fert. Tech. 18 (1981) 140.
[12] R.W. Bedford, ICI Technical Paper No. 4., Imperial Chemical Industries, Billingham, Cleveland, UK.
[13] J.S. Campbell, Ind. Eng. Chem. Proc. Des. Dev. 9 (1970) 588.
[14] M.J. L Ginés, N. Amadeo, M. Laborde, C.R. Apesteguia, Appl. Catal. A 131 (1995) 283.
[15] T. Shido, Y. Iwasawa, J. Catal. 140 (1993) 575.
[16] F. Garbassi, G. Petrini, J. Catal. 90 (1984) 106.
[17] A Andreev, T Haltchev, V Kafedjiiski, B. Kunev, M. Kalchev, I. Orizarski, D. Shopov, Proceedings of the Sixth International Symposium, Heterogeneous Catalysis, Part 1, Sofia, 1987, p. 235.
[18] W.L. Marsden, M.S. Wainwright, J.B. Friedrich, Ind. Eng. Chem. Prod. Res. Dev. 19 (1980) 551.
[19] M. Raney, US Patent Nr. 1, 563 587.
[20] L. Fauconnau, Bull. Soc. Chem. 5 (1937) 58.
[21] M.S. Wainwright, R.B. Anderson, J. Catal. 64 (1980) 124.
[22] M.S. Wainwright, D.L. Trimm, Catal. Today 23 (1995) 29.
[23] H.E. Curry-Hyde, M.S. Wainwright, D.J. Young, Appl. Catal. 77 (1991) 75.
[24] H.E. Curry-Hyde, M.S. Wainwright, D.J. Young, Appl. Catal. 77 (1991) 89.
[25] H.E. Curry-Hyde, M.S. Wainwright, D.J. Young, in: D.M. Bibby, C.D. Chang, R.F. Howe, S. Yurchak (Eds.), Methane Conversion, Elsevier, Amsterdam, 1988, p. 239.
[26] J.B. Friedrich, D.J. Young, M.S. Wainwright, J. Electrochem. Soc. 128 (1981) 1840.
[27] L.F. Mondolfo, Aluminium Alloys: Structures and Properties, Butterworths, London, 1976.
[28] J.B. Friedrich, D.J. Young, M.S. Wainwright, J. Electrochem. Soc. 128 (1981) 1845.
[29] A.B. Stiles, Catalyst Manufacture Laboratory and Commercial Preparations, Marcel Dekker, New York and Basel, 1983, p. 118.
[30] J.W. Evans, M.S. Wainwright, A.J. Bridgewater, D.J. Young, Appl. Catal. 7 (1983) 75.
[31] J.R. Mellor, Ph.D. Thesis, University of the Witwatersrand, Johannesburg, South Africa, 1993.
[32] J.R. Anderson, K.C. Pratt, Introduction to Characterisation and Testing of Catalysts, Academic Press, New York, 1985.
[33] J.M. Thomas, J.W. Thomas, Introduction to the Principles of Heterogeneous Catalysis, Academic Press, New York, 1975, p. 16.
[34] A.D. Tomsett, H.E. Curry-Hyde, M.S. Wainwright, D.J. Young, A.J. Bridgewater, Appl. Catal. 33 (1987) 119.
[35] A. Andreev, V. Kafedjiiski, T. Halacher, B. Kunev, M. Kaltchev, Appl. Catal. 78 (1991) 199.
[36] M.S. Wainwright, D.J. Young, A.J. Bridgewater, Commonwealth of Australia National Energy Research, Development and Demonstration Program, Report No. 376 (1984).
[37] J.B. Friedrich, D.J. Young, M.S. Wainwright, J. Catal. 80 (1983) 14.
[38] A.J. Bridgewater, M.S. Wainwright, D.J. Young, J.P. Orchard, Appl. Catal. 7 (1983) 369.
[39] T. van Herwijnen, W.A. de Jong, J. Catal. 34 (1974) 209.
[40] A.D. Tomsett, M.S. Wainwright, D.J. Young, Appl. Catal. 12 (1984) 43.
[41] J.H. de Boer, in: D.H. Everett, F.S. Stone (Eds.), Structure and Properties of Porous Materials, Butterworths, London, 1958, p. 68.
[42] N.I. Onuoho, A.D. Tomsett, M.S. Wainwright, D.J. Young, J. Catal. 91 (1985) 25.
[43] A.D. Tomsett, D.J. Young, M.S. Wainwright, Appl. Catal. 35 (1987) 321.
[44] F. Chongzheng, M.S. Wainwright, D.L. Trimm, Appl. Catal. 54 (1989) 53.
[45] F. Chongzheng, W. Changsui, W. Shengjun, Wi. Youshi, D.L. Trimm, M.S. Wainwright, Chin. Chem. Lett. 1 (1990) 279.
[46] J.B. Friedrich, M.S. Wainwright, D.J. Young, J. Catal. 80 (1983) 1.
[47] A.D. Tomsett, D.J. Young, M.R. Stammbach, M.S. Wainwright, J. Mat. Sci. 25 (1990) 4106.
[48] S. Durbach, J. Mellor, N.J. Coville, T.E. Derry, Nuclear Instruments and Methods in Physics Research B80/81 (1993) 294.
[49] J.R. Mellor, N.J. Coville, A.C. Sofianos, R.G. Copperthwaite, Appl. Catal. A (1997).